Journal of The Electrochemical Society, **155** (3) J71-J78 (2008)
0013-4651/2008/155(3)/J71/8/$23.00 © The Electrochemical Society

Synthesis and Luminescence Properties of Intensely Red-Emitting $M_5Eu(WO_4)_{4-x}(MoO_4)_x$ (M = Li, Na, K) Phosphors

Chuang-Hung Chiu,[a] Chih-Hsuan Liu,[b] Sheng-Bang Huang,[b] and Teng-Ming Chen[a,z]

[a]*Phosphors Research Laboratory, Department of Applied Chemistry, National Chiao Tung University, Hsinchu 30010, Taiwan*
[b]*Electronics and Opto-electronics Research Laboratories, Industrial Technology Research Institute, Hsinchu 30010, Taiwan*

We have investigated the luminescence of a series of $M_5Eu(WO_4)_{4-x}(MoO_4)_x$ (M = Li, Na, K) phosphors and discovered that $Na_5Eu(WO_4)_{4-x}(MoO_4)_x$ ($0 \le x \le 4.0$) exhibit the most intense red emission among the three investigated. Powder X-ray diffraction investigations show that a complete solid solution can be formed in the indicated composition range. The effect of chemical compositions on the luminescence properties of $Na_5Eu(WO_4)_{4-x}(MoO_4)_x$ has been investigated and discussed. The Commission International de l'Eclairage chromaticity coordinates were found to be (0.66,0.33) for $Na_5Eu(WO_4)_{4-x}(MoO_4)_x$, which reaches the same level as that of the $Y_2O_2S:Eu^{3+}$ commodity. The color-rendering index (Ra) of a typical white-light–light emitting diode (WL-LED) based on $Na_5Eu(WO_4)_2(MoO_4)_2$ was found to be 82.3, higher than that (i.e., $Ra \sim 70.8$) obtained for the WL-LED fabricated using the commodity of $La_2O_2S:Eu^{3+}$ when the WL-LEDs were operated at a forward-bias current (I_f) of 20 mA at room temperature. $Na_5Eu(WO_4)_{4-x}(MoO_4)_x$ is therefore suggested to be a potential red-emitting phosphor for WL-LED.
 [DOI: 10.1149/1.2825178]

Manuscript submitted August 31, 2007; revised manuscript received November 12, 2007. Available electronically January 8, 2008.

Light emitting diodes (LEDs) have received much attention for their potentiality of being used as general lighting devices. The development of white color is extremely significant to expand LED applications toward general lighting.[1] White-light (WL) LEDs offer benefits in accordance with stability, energy savings, perpetuation, and safety. There are three important methods for a single-chip WL-LED.[2] The most predominant WL-LED uses a 450–470 nm blue-emitting LED that excites a yellow-emitting $Y_3Al_5O_{12}:Ce^{3+}$ ($YAG:Ce^{3+}$) phosphor dispersed in the epoxy resin on a blue LED chip.[3] This method is presently the most efficient technique. However, the light color is not truely white due to the deficient red component. Therefore, the importance of blue-excitable red-emitting phosphor is increasing. The second method is to combine a blue chip with the blue-excitable red- and green-emitting phosphors. The third option is to set three phosphors (red-, green-, and blue-emitting) that down-convert the near-UV/blue light into visible light on LED chip. Notably, the red light-emitting phosphors for WL-LED based on near-UV/blue chip is still limited commercially to sulfide-based materials, such as $CaS:Eu^{2+}$, $SrY_2S_4:Eu^{2+}$, and ZnCdS:Cu,Al.[4,5] However, there are certain disadvantages to use those sulfide-based materials, such as chemical instability, large spectral full width at half maximum, and low efficiency.[6]

Hence, there has been a widespread and growing interest in developing new families of red-emitting phosphors with high absorption in the near UV to blue region. The luminescence properties of rare-earth molybdates and tungstates have long attracted the attention of investigators.[7] A number of patents represent almost all combinations between rare-earth oxides and molybdenum and tungsten trioxides activated by Eu^{3+} and Tb^{3+}, including compositions that are not in accord with the stoichiometry of presently known compounds.[8-11] Trunov et al. reported the synthesis and crystallographic data of $Na_5Ln(MoO_4)_4$ and $Na_5Ln(WO_4)_4$, where Ln represents the rare-earth ions in 3+ oxidation state, and the same group of researchers also studied the luminescence spectra of $Na_5Ln(MoO_4)_4$ and $Na_5Ln(WO_4)_4$ in 1978.[12] The luminescence properties of double molybdates and tungstates of rare earths and alkali metals were described by Dzhurinskii et al.[7] In addition, fluorescence spectra for polycrystalline $Na_5Eu(MO_4)_4$ (M = Mo, W) samples have been measured and analyzed at 4.2, 77, and 300 K, respectively, and their crystal field calculations have also been performed by Huang et al.[13]

The crystal structure of $Na_5Y(MoO_4)_4$, isostructural with $Na_5Ln(MoO_4)_4$ and reported to be scheelite related with all the tetrahedral sites occupied by an ordered arrangement of Mo and Na in 4:1 ratio,[14] have been determined from single-crystal X-ray diffraction (XRD) data [space group $I4_1/a$, $Z = 4$, $a = 11.374(3)$ Å, $c = 11.440(5)$ Å] Recently, Wang et al. investigated the photoluminescence (PL) properties of $Na_5La(MoO_4)_4:xEu^{3+}$ and $NaEu(MoO_4)_2$.[15] Bright red-light emitting diodes were fabricated by coating the phosphors onto near-UV-emitting InGaN chips, respectively, and the diodes prepared with phosphor $Na_5Eu(MoO_4)_4$ show good Commission International de l'Eclairage (CIE) chromaticity and exhibit more intense red emission than that fabricated with $NaEu(MoO_4)_2$. Neeraj et al. reported a series of intensely luminescent red-emitting $NaM(MoO_4)_{2-x}(WO_4)_x$ (M = Gd, Y, Bi) phosphors that can be excited at ~394 nm attributed to the sharp $^7F_0$-$^5L_6$ absorption of Eu^{3+}.[16]

Motivated by the above-stated investigations and the attempts to develop phosphors excitable by near-UV and/or blue radiation for the applications of WL-LED, we have systematically investigated and reported herein the preparation, PL, and color chromaticity properties of a series of phosphors with composition $Na_5Eu(WO_4)_{4-x}(MoO_4)_x$ ($0 \le x \le 4.0$), whose compositions are different from those reported by Sivakumar et al.,[6] Wang et al.,[15] and Neeraj et al.[16] By using the composition-optimized $Na_5Eu(WO_4)_2(MoO_4)_2$ phosphor, we have also fabricated a WL-LED whose performance was compared to that of a WL-LED fabricated based on the commonly used commodity of $La_2O_2S:Eu^{3+}$.

Experimental

The phosphors of the compositions $M_5Eu(WO_4)_{4-x}(MoO_4)_x$ were synthesized by high-temperature solid-state reactions. The starting materials used were M_2MoO_4 (99.9%; M=Li, Na, K) (Strem Chemicals, Newburyport, MA, USA), M_2WO_4 (99.9%; M=Li, Na, K), MoO_3 (99.95%), WO_3 (99.9%), (all from Cerac Chemicals, Milwaukee, Wisconsin, USA) and Eu_2O_3 (99.99%, Aldrich Chemicals, Milwaukee, Wisconsin, USA). Stoichiometric amounts of reactants were ground by ballmilling and then heated at 600°C for 6 h. The XRD profiles were recorded by using a Bruker D8 Advanced diffractometer equipped with Cu Kα radiation (λ

[z] E-mail: tmchen@mail.nctu.edu.tw

= 1.5418 Å) operated at 40 kV and 40 mA. XRD data for phase identification were collected in a 2θ range from 10 to 80° with a step interval of 0.100°/1.5 s. The measurements of PL and PL excitation (PLE) spectra were performed by using a Spex Fluorolog-3 spectrofluorometer (Instruments S.A., Edison, N.J., USA) equipped with a 450 W Xe light source and double excitation monochromators. The powder samples were compacted and excited under 45° incidence, and emitted fluorescence was detected by a Hamamatsu Photonics R928 type photomultiplier perpendicular to the excitation beam. The spectral response of the measurement system is calibrated automatically on startup. To eliminate the second-order emission of the source radiation, a cutoff filter was used in the measurements.

Diffuse reflectance spectra of phosphor samples were measured with a Hitachi 3010 double-beam UV-visible (vis) spectrometer (Hitachi Co., Tokyo, Japan) equipped with a ø60 mm integrating sphere whose inner face was coated with $BaSO_4$ or Spectralon, and α-Al_2O_3 was used as a standard in the measurements. The CIE chromaticity coordinates for all samples were determined by a Laiko DT-100 color analyzer equipped with a charge coupled device (CCD) detector (Laiko Co., Tokyo, Japan). The scanning electron microscope (SEM) images were measured with a Hitachi S-4000 field-emission-type SEM with operation voltage in the range of 0.5–30 kV.

To compare the performance of composition-optimized phosphor $Na_5Eu(WO_4)_2(MoO_4)_2$ and that of commodity phosphor $La_2O_2S:Eu^{3+}$ (Kasei Optonix KX-681B) in the fabrication of WL-LEDs, phosphor-converted WL-LEDs were fabricated. Based on the standard LED technology, one WL-LED was achieved by using an n-UV LED chip (average λ_{em} = 392 nm, Cree catalog no. C395MB290-S0100) in pumping blue-emitting $BaMgAl_{10}O_{17}:Eu^{2+}$ (Kasei optonix KX-661), green-emitting (Ba,Sr)-Si-Al-O:Eu^{2+},Dy^{3+} (Nantex RU-G534), and our red-emitting $Na_5Eu(WO_4)_2(MoO_4)_2$ phosphors simultaneously. The above-mentioned $BaMgAl_{10}O_{17}:Eu^{2+}$ and (Ba,Sr)-Si-Al-O:Eu^{2+},Dy^{3+} phosphors were excellent commodities because of their nonoxicity, thermal stability, and intense luminescence properties. The phosphors were encapsulated in a transparent epoxy resin (KBIN A2015). The second WL-LED, based on $La_2O_2S:Eu^{3+}$ commodity, was also fabricated at the same collocation for comparison. The optimal weight ratio of $R(Na_5Eu(WO_4)_2(MoO_4)_2)$-G-B phosphors was 0.93:0.06:0.01, whereas that for $R(La_2O_2S:Eu^{3+})$-G-B phosphors combination was 0.69:0.23:0.08. This ratio changes depended on the target color of white region. The relative emission spectra of n-UV chip WL-LED based on $Na_5Eu(WO_4)_2(MoO_4)_2$ and $La_2O_2S:Eu^{3+}$ at room temperature and a I_f of 20 mA were measured using a 50 cm single-grating monochromator.

Results and Discussion

The XRD investigation results and comparison of the powder XRD profiles of $M_5Eu(MoO_4)_4$ (M = Li, Na, K) phases are represented in Fig. 1. All of the as-prepared compounds were found to be single phased. The XRD profiles of $M_5Eu(MoO_4)_4$ (M = Na, K) were discovered to be in good agreement with those studied earlier and reported in JCPDS 82-2368 [$Na_5Y(MoO_4)_4$] and JCPDS 45-0340 [$K_5Eu(MoO_4)_4$]. The two kinds of alkali-metal rare-earth-meta1 molybdates described above were found to crystallize in the tetragonal and hexagonal crystal systems, respectively. For $Li_5Eu(MoO_4)_4$, no similar structural data of the compound can be found for comparison despite the high level of interest in the optical properties of the material. We therefore undertook a study on the luminescence of $M_5Eu(WO_4)_{4-x}(MoO_4)_x$ (M = Li, Na, K) phosphors, beginning our work at a time when no $M_5Eu(MoO_4)_4$ compounds had been fully characterized.

Figure 2 shows the powder XRD patterns of $Na_5Eu(WO_4)_{4-x}(MoO_4)_x$ (x = 0, 1, 2, 3, 4) phases as a function of

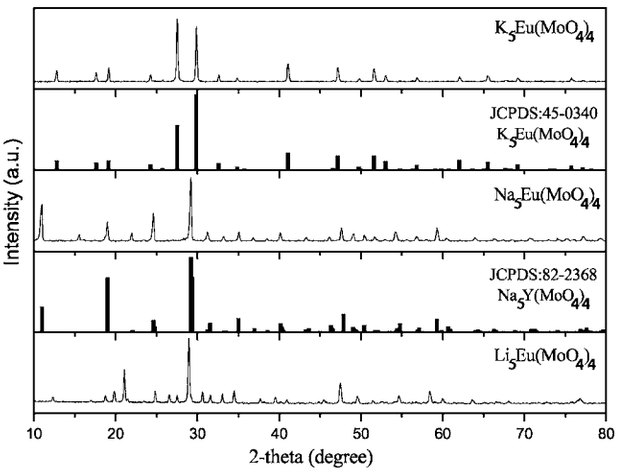

Figure 1. Powder XRD patterns of $M_5Eu(MoO_4)_4$ (M = Li, Na, K).

substituted Mo content. The crystal structure of all single-phased samples were found to be similar to that of $Na_5Y(WO_4)_4$ [JCPDS 82-0410, space group $I4_1/a$, $Z = 4$, a = 11.447(7) Å, c = 11.336(1) Å].[17] When the tungstate group is substituted by molybdate group, the XRD profiles were found to be similar without showing discernible shifting, which can be rationalized by the almost identical ionic radius of Mo^{6+} and W^{6+}. We have also carried out an XRD cell parameter refinement based on the diffraction peaks obtained from the XRD profiles of $Na_5Eu(WO_4)_{4-x}(MoO_4)_x$ using the scheelite-related structure of $Na_5Y(WO_4)_4$,[17] and the results are summarized in Fig. 3. Our data show that as x increases, the cell parameters a and b decreases marginally, whereas c increases systematically, indicating that a solid solution is very likely to form between end members $Na_5Eu(WO_4)_4$ and $Na_5Eu(MoO_4)_4$ in the series of $Na_5Eu(WO_4)_{4-x}(MoO_4)_x$. Similar research results have also been witnessed by Sivakumar and Varadaraju in the $AgLa_{0.95}Eu_{0.05}(WO_4)_{2-x}(MoO_4)_x$ (x = 0–2) system, and they confirmed that minor distortions in the crystal structure play a crucial role in determining the luminescence properties in these systems.[18]

To investigate and optimize the effect of alkali-metal ion doping on the luminescence of $M_5Eu(WO_4)_{4-x}(MoO_4)_x$ (M = Li, Na, K), we have made an attempt to synthesize, study, and compare the PL spectra of $M_5Eu(MoO_4)_4$ with M being isovalent Li^+, Na^+, and K^+

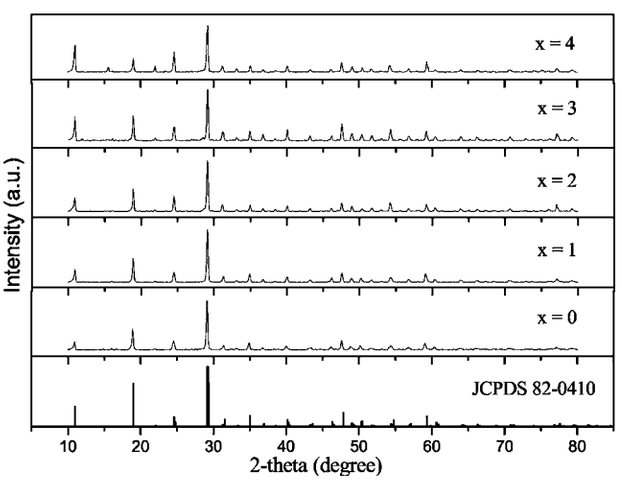

Figure 2. Powder XRD patterns of $Na_5Eu(WO_4)_{4-x}(MoO_4)_x$ (x = 0, 1, 2, 3, 4) and $Na_5Y(WO_4)_4$ (JCPDS 82-0410).

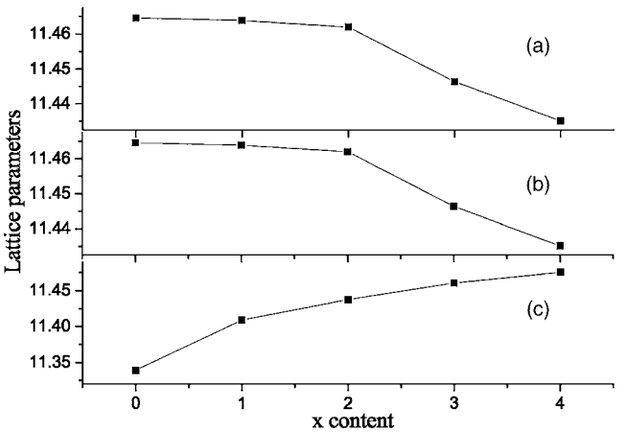

Figure 3. Cell parameters as a function of x for $Na_5Eu(WO_4)_{4-x}(MoO_4)_x$ phosphors.

cations, respectively. The PLE and PL spectra of selected compositions of $M_5Eu(MoO_4)_4$ (M = Li, Na, K) were shown in Fig. 4 and 5, respectively. In Fig. 4, the excitation intensity of PLE spectra was found to reach a maximum by isovalent substitution with Na^+, regardless of the size of alkali cations. Similarly, a condition in the variation of PL spectra of three phosphors has also been observed. We were incapable of organizing the relation between luminescence properties of the compounds and the type of the alkali cation within a given type of double salts because changing the cation usually causes a concomitant change in the structure of the compound.[7] The relation between luminescence properties and crystal structure of the compounds (the degree of ordering of cation in lattice) is not solitary.[19]

As shown in Fig. 6, the PLE spectra of five molybdotungstate samples with selected compositions of $Na_5Eu(WO_4)_{4-x}(MoO_4)_x$ (x = 0,1, 2, 3, 4) were measured in the spectral range from 200 to 590 nm by monitoring the emission at 616 nm that is attributed to $^5D_0 \rightarrow {}^7F_2$ transition of Eu^{3+} ions. The intense broadband appears at 280 nm and is assigned as the charge-transfer (CT) transition between oxygen and tungsten or molybdenum (i.e., ligand to metal charge-transfer).[6] Nevertheless, the charge-transfer band of Eu^{3+}–O^{2-} was not definitely observed in the PLE spectra, which could presumably be due to possible overlap of the CT band with that of tungstate or molybdate group. In the spectral region from 350 to 550 nm, all five $Na_5Eu(WO_4)_{4-x}(MoO_4)_x$ samples show characteristic intraconfigurational 4f–4f emissive transitions of Eu^{3+}: sharp $^7F_0 \rightarrow {}^5L_6$ transition for 394 nm, $^7F_0 \rightarrow {}^5D_2$ transition for 465 nm,

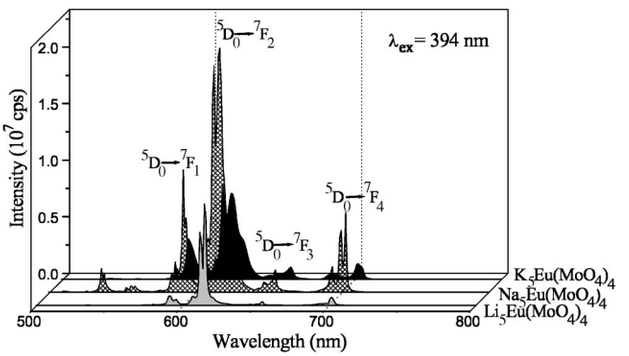

Figure 5. Comparison of PL spectra for phosphors of $M_5Eu(WO_4)_{4-x}(MoO_4)_x$ (M = Li, Na, K).

and the $^7F_1 \rightarrow {}^5D_1$ transition for 535 nm. As compared to the CT band, remarkable changes were observed in the intensity of characteristic absorptions of Eu^{3+} ion in the PLE spectra shown in Fig. 6, and the maximum absorption peak attributed to Eu^{3+} $^7F_0 \rightarrow {}^5L_6$ becomes stronger when the occupancies of W/Mo sites were found at 50%/50%.

Figure 7 shows the emission spectra of $Na_5Eu(WO_4)_{4-x}(MoO_4)_x$ (x = 0, 1, 2, 3, 4) under near-UV excitation at 394 nm. The spectra essentially consist of sharp lines with wavelength ranging from 580 to 720 nm, which are associated with the $^5D_0 \rightarrow {}^7F_J$ (J = 1, 2, 3, 4) transitions from the excited levels of Eu^{3+} to the ground state, but no emission corresponding to tungstate or molybdate is observed. Notwithstanding the presence of an absorption band from the tungstate or molybdate group in the excitation spectra of Eu^{3+} by monitoring the emission at 616 nm, it clearly suggests that the energy absorbed by the WO_4^{2-}/MoO_4^{2-} group is transferred to Eu^{3+} levels nonradiatively. This process has been known as "host-sensitized",[20,21] energy transfer. However, the intensity of Eu^{3+} emission is weaker with CT band excitation when compared to that due to Eu^{3+} excitation.[6] This reveals that the energy transfer from the W/Mo–O CT states to 4f levels of Eu^{3+} is not efficient.

As indicated in Fig. 7, the strongest emission peak located at 616 nm, which is due to that Eu^{3+} ion occupying the lattice site without inversion symmetry. The result agrees with the data of its crystal structure.[14,15] The presence of multiplets in the emission spectra are attributed to the $(2J + 1)$ Stark components of J-degeneracy splitting. The $^5D_0$ is the unsplitted singlet band, simplifying in a significant way the application of the group theory and of electronic transition selection rules. Without inversion symmetry at Eu^{3+} lattice site, the electric-dipole transition would be dominant.

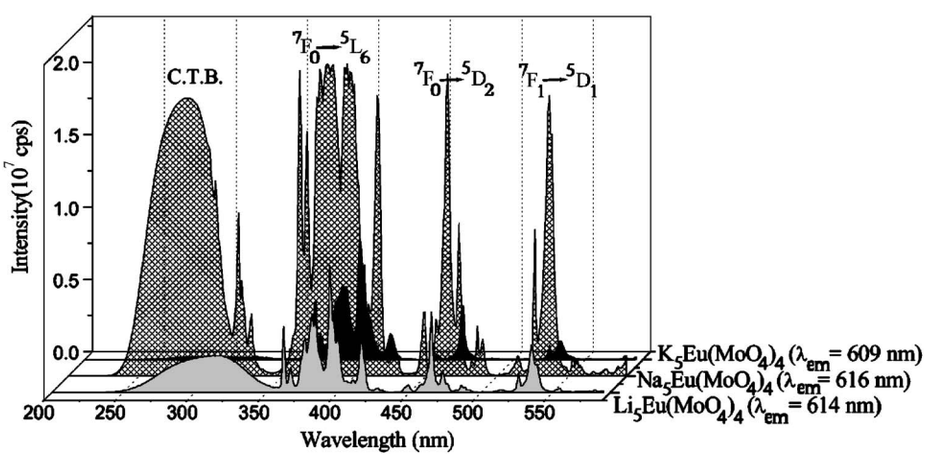

Figure 4. Comparison of PLE spectra for phosphors of $M_5Eu(WO_4)_{4-x}(MoO_4)_x$ (M = Li, Na, K).

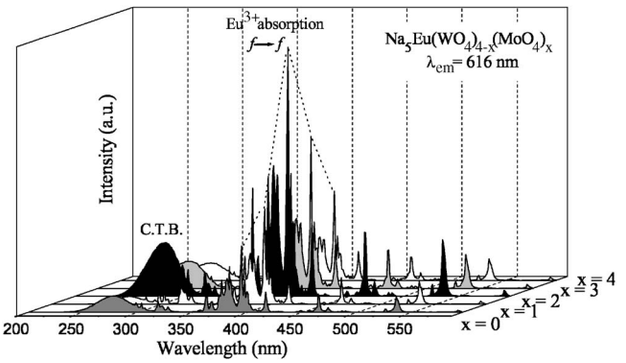

Figure 6. PLE spectra monitored at 616 nm for $Na_5Eu(WO_4)_{4-x}(MoO_4)_x$ phosphors with x = 0, 1, 2, 3, and 4.

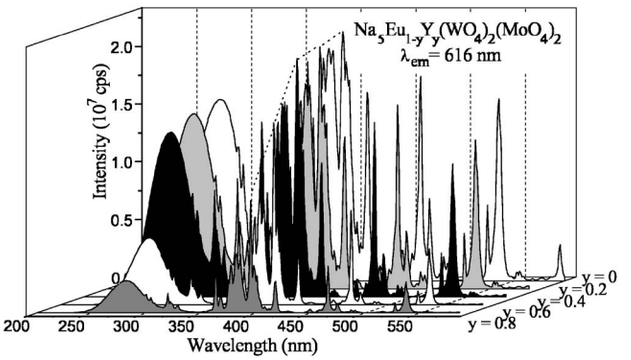

Figure 8. PLE spectra of the $Na_5Eu_{1-y}Y_y(WO_4)_2(MoO_4)_2$ system by varying the Y^{3+}-diluting concentration.

For this reason, the intensity of $^5D_0 \rightarrow {}^7F_{2,4}$ (electric-dipole transition) was found to be much stronger than that of $^5D_0 \rightarrow {}^7F_{1,3}$ (magnetic-dipole transition). The major emission of $Na_5Eu(WO_4)_{4-x}(MoO_4)_x$ was found at 616 nm ($^5D_0 \rightarrow {}^7F_2$), which corresponds to red emission. Other transitions of Eu^{3+} from the ^5D_J excited levels to ^7F_J ground states, for instance, $^5D_0 \rightarrow {}^7F_J$ is located at 570–720 nm and the $^5D_1 \rightarrow {}^7F_J$ transitions located at 520–570 nm are both very weak, and therefore, the more saturated CIE chromaticity benefited greatly by the reasoning. In addition, the intensity of $^5D_0 \rightarrow {}^7F_2$ transition reaches a maximum when the relative ratio of W/Mo is 1:1. The reason for this interesting observation may be due to the advent of ion pair interaction between Eu^{3+} ions, which is expected to be much stronger when W/Mo occupied bisection of the lattice sites separately. Similar observation to change W/Mo relative ratio has also been witnessed by Sivakumar and Varadaraju in the $AgLa_{0.95}Eu_{0.05}(WO_4)_{2-x}(MoO_4)_x$ (x = 0–2) system.[18]

To research whether concentration quenching has existed or not, the variation of the PL intensity with Y^{3+}-concentration has been investigated for $Na_5Eu_{1-y}Y_y(WO_4)_2(MoO_4)_2$ (y = 0, 0.2, 0.4, 0.6, 0.8). The PLE and PL spectra of the compounds $Na_5Eu_{1-y}Y_y(WO_4)_2(MoO_4)_2$ with different Y^{3+}-concentrations were shown in Fig. 8 and 9, respectively. The compound $Na_5Eu(WO_4)_2(MoO_4)_2$ (i.e., y = 0) shows the maximum PL intensity under 394 nm excitation. There is no concentration quenching of luminescence for our study. In 1988, Pan et al. reported that the compound $Na_5Eu(WO_4)_4$ did not exhibit concentration quenching because of the special structure of it.[22] The bond angles of O–W–O and Eu–O–W are 105 and 100°, respectively, which reveal great difficulty for energy transfer between Eu^{3+} ions to occur. Our results are in good agreement with that reported by Pan et al.,[22] and thus, $Na_5Eu(WO_4)_2(MoO_4)_2$ has also been proved to be a good phosphor showing no concentration quenching.

To investigate the optical properties of $Na_5Eu(WO_4)_{4-x}(MoO_4)_x$ phosphors, we have also measured their DR spectra as a function of x and the results are represented in Fig. 10. From the evolution of the DR spectra, the observed absorption band centering at 270 nm tends to shift toward longer wavelengths with increasing doped Mo content or x value. Furthermore, in almost all of the phosphors with varied x values, we have observed several absorptions at 270–330

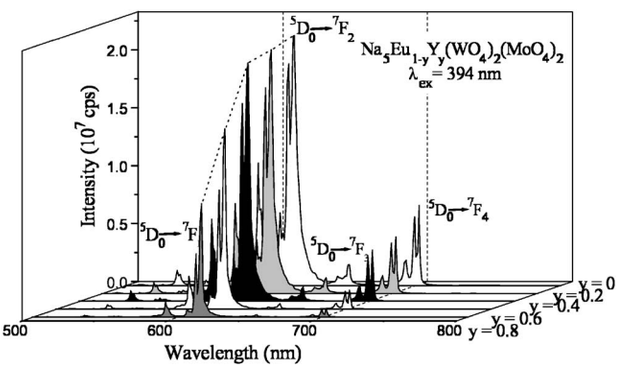

Figure 9. PL spectra of the $Na_5Eu_{1-y}Y_y(WO_4)_2(MoO_4)_2$ system by varying the Y^{3+}-diluting concentration under 394 nm excitation wavelength.

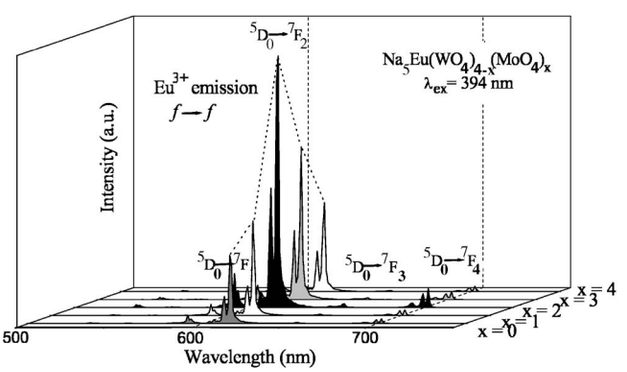

Figure 7. PL spectra of $Na_5Eu(WO_4)_{4-x}(MoO_4)_x$ (x = 0, 1, 2, 3, 4) under 394 nm near-UV excitation.

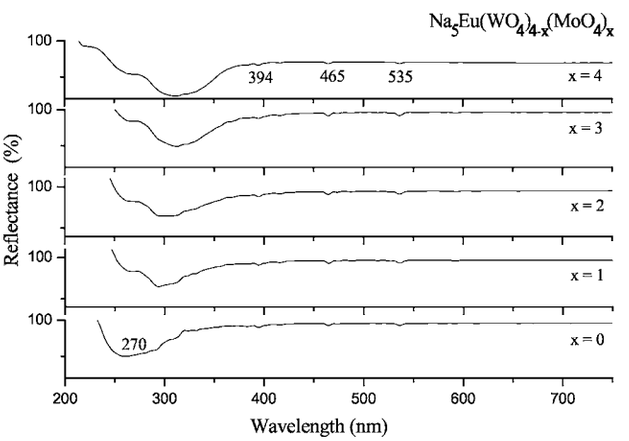

Figure 10. Diffuse reflectance spectra of $Na_5Eu(WO_4)_{4-x}(MoO_4)_x$ phosphors as a function of Mo content (x).

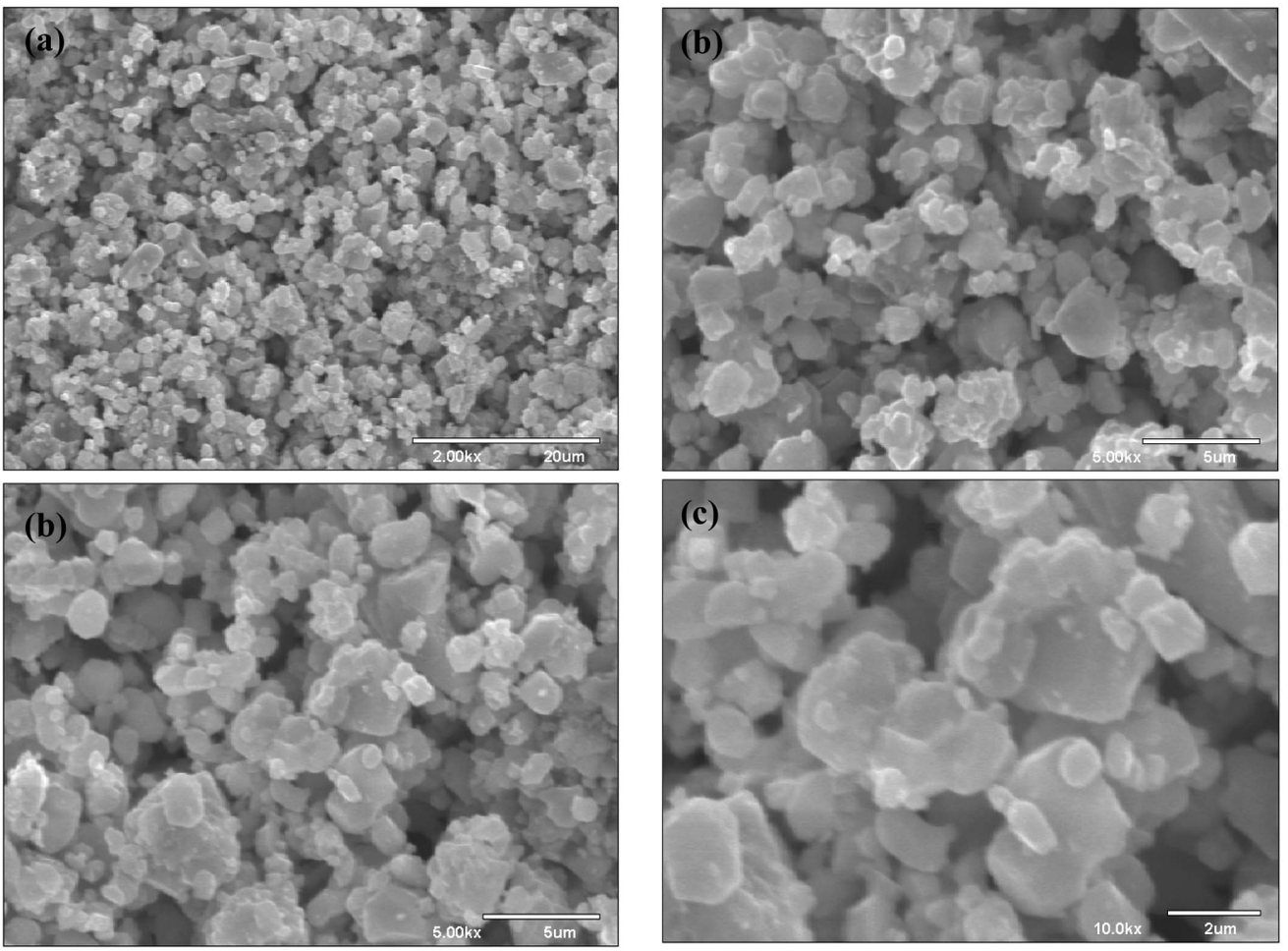

Figure 11. SEM micrographs (a) 2000×, (b) 5000×, and (c) 10,000× of polycrstalline samples of $Na_5Eu(WO_4)_2(MoO_4)_2$.

[attributed to charge-transfer transition O 2p → Mo(W)(4d(5d))], 394 ($^7F_0 \rightarrow {}^5L_6$), 465 ($^7F_0 \rightarrow {}^5D_2$), and 535 ($^7F_1 \rightarrow {}^5D_1$) nm, which were found to be consistent with those observed in the PLE spectra (shown in Fig. 6) and discussed previously.

In addition, from the SEM image analysis, we have observed that the $M_5Eu(WO_4)_2(MoO_4)_2$ (M = Li, Na, K) phosphors prepared show well-defined aggregated but irregular grains with dimension of <10 μm. The irregular particle morphology observed reveals the inherent characteristics of the adopted solid-state method (see Fig. 11 and 12).

From a practical application point of view, the color chromaticity of phosphors is considered to be critical parameters for evaluating the performance of LED phosphors. The CIE color coordinates (x,y) and relative luminance of the our red-emitting phosphors investigated in this work are reported and compared against those of the commodity $Y_2O_2S:Eu^{3+}$ (Kasei Optonix P22-RE3, λ_{ex} = 342 nm, PLE and PL spectra were illustrated in Fig. 13) and $La_2O_2S:Eu^{3+}$ (Kasei Optonix KX-681B, λ_{ex} = 394 nm, PLE and PL spectra were illustrated in Fig. 14) in Table I. For the series of $Na_5Eu(WO_4)_{4-x}(MoO_4)_x$ phosphors with different W/Mo ratios, the experimental CIE (x,y) coordinates were found to be (0.66, 0.33) for all compounds with different x's and it has reached the same level as the Kasei's commodity of $Y_2O_2S:Eu^{3+}$. The CIE chromaticity coordinates of $Na_5Eu(WO_4)_{4-x}(MoO_4)_x$ approach that of the NTSC red [i.e., (0.67,0.33)]. In addition, we also found that with changing the relative ratio of W/Mo the relative luminance changes from 1.8 (x = 0) to 1.3 (x = 4) and the optimal luminance was observed to be 2.5 (x = 2). The relative luminance value of $Na_5Eu(WO_4)_{4-x}(MoO_4)_x$ was found to be larger than either $Y_2O_2S:Eu^{3+}$ or $La_2O_2S:Eu^{3+}$. Accordingly, our investigation results indicate that $Na_5Eu(WO_4)_{4-x}(MoO_4)_x$ is exceptionally attractive as a near-UV convertible phosphor as compared to the conventional $Y_2O_2S:Eu^{3+}$ and $La_2O_2S:Eu^{3+}$ in the application as a red-emitting phosphor for LEDs.

WL-LEDs were fabricated by precoating blue, green, and red phosphors onto n-UV LED chips, previously packaging them into LED lamps. Figure 15 shows the comparison of emission spectra of the WL-LEDs based on an n-UV chip, $Na_5Eu(WO_4)_2(MoO_4)_2$, and $La_2O_2S:Eu^{3+}$ and corresponding blue- and green-emitting phosphors at a I_f of 20 mA, respectively, where $La_2O_2S:Eu^{3+}$ is a commonly used commercial red phosphor for WL-LED application today. Essentially, three bands were observed in the LED emission spectra and the strong sharp peak located at 392 nm came from the n-UV LED chip directly. The broad EL band located at 430–575 nm was originated from the blue and green phosphors, and the sharp emission peaks located at 580–720 nm originated from the red phosphor, respectively. The phenomenon of a short-wavelength emission peak shows that near-UV light emitted from the LED chips was not completely absorbed by the precoated phosphors in LED lamps. It is also well known that down-conversion efficiency depends strongly on phosphor composition and phosphor grain size.[23]

For the WL-LED based on $Na_5Eu(WO_4)_2(MoO_4)_2$, color tem-

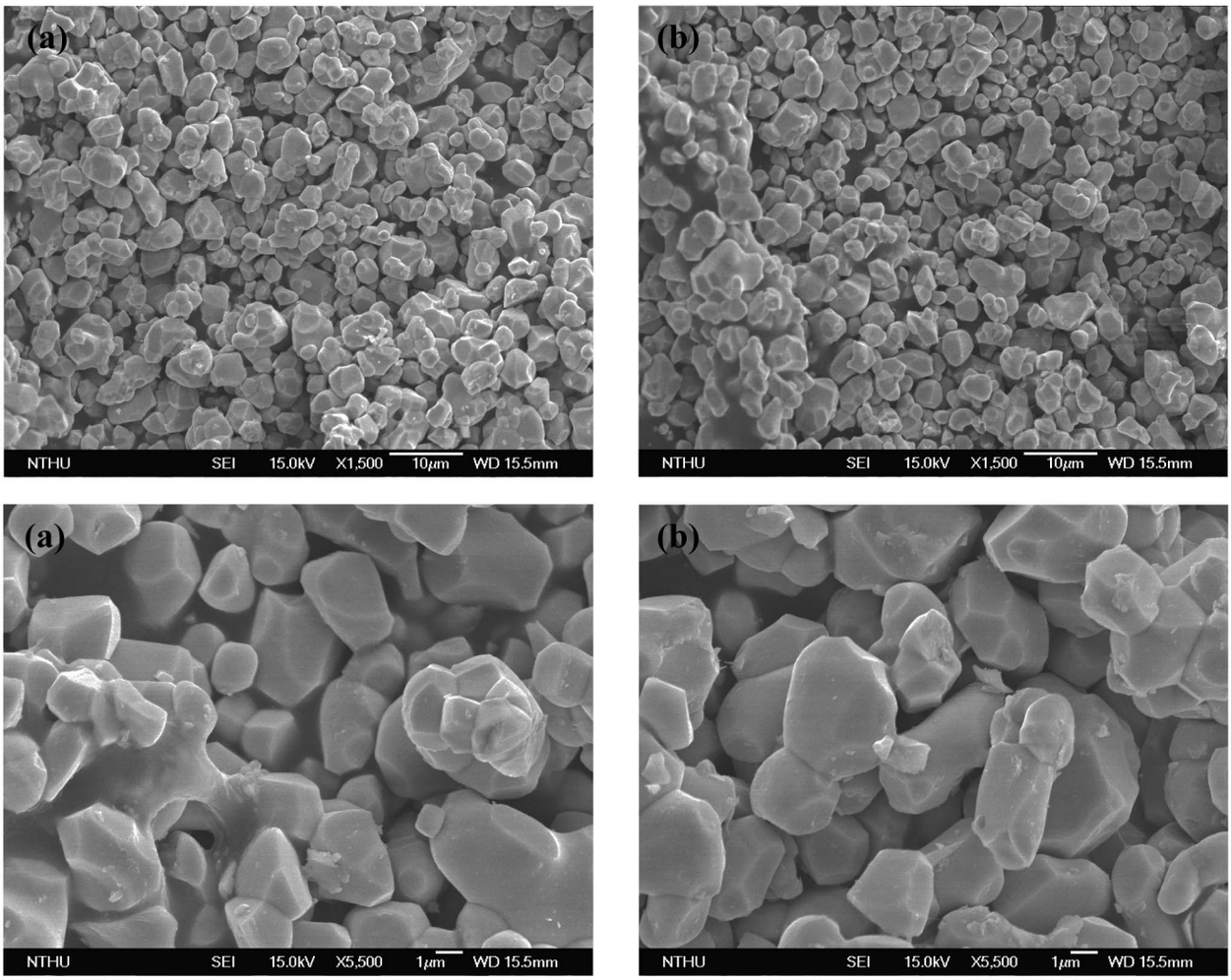

Figure 12. SEM micrographs of (a) $Li_5Eu(WO_4)_2(MoO_4)_2$ and (b) $K_5Eu(WO_4)_2(MoO_4)_2$ phosphors.

perature (T_{cp}) and the luminous efficacy (η_L) were found to be 7491 K and 10 lm/W when the WL-LED was operated at a I_f of 20 mA at room temperature. For the other WL-LED based on $La_2O_2S:Eu^{3+}$, T_{cp} and η_L were found to be 6782 K and 10 lm/W,

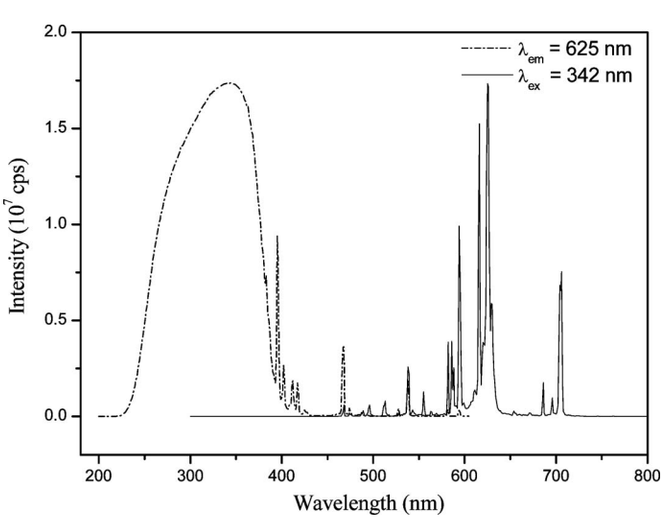

Figure 13. PLE and Pl spectra for the commercially available $Y_2O_2S:Eu^{3+}$.

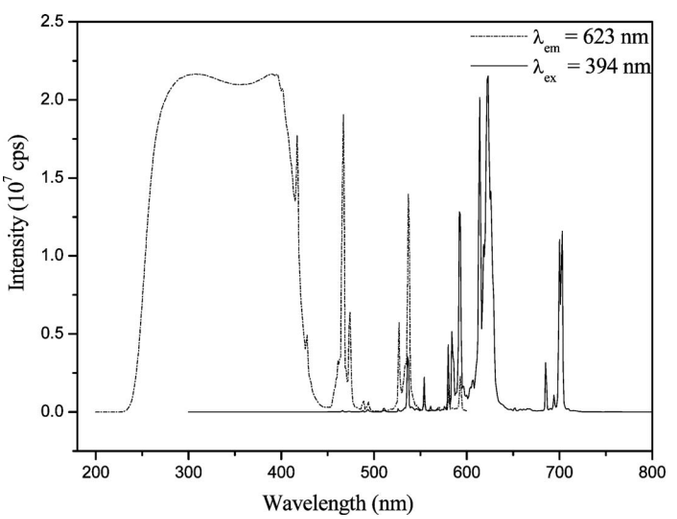

Figure 14. PLE and Pl spectra for the commercially available $La_2O_2S:Eu^{3+}$.

Table I. Comparison of CIE chromaticity coordinates of phosphors investigated in the work (λ_{ex} = 394 nm for $Na_5Eu(WO_4)_{4-x}(MoO_4)_x$ and $La_2O_2S:Eu^{3+}$; λ_{ex} = 342 nm for $Y_2O_2S:Eu^{3+}$).

Phosphor compositions	CIE color coordinates (x,y)	Relative luminance (a.u.)
$Na_5Eu(WO_4)_4$	(0.66,0.33)	1.8
$Na_5Eu(WO_4)_3(MoO_4)_1$	(0.66,0.33)	1.8
$Na_5Eu(WO_4)_2(MoO_4)_2$	(0.66,0.33)	2.5
$Na_5Eu(WO_4)_1(MoO_4)_3$	(0.66,0.33)	2.2
$Na_5Eu(MoO_4)_4$	(0.66,0.33)	1.3
$Li_5Eu(MoO_4)_4$	(0.67,0.32)	1.2
$K_5Eu(MoO_4)_4$	(0.66,0.33)	1.1
$Y_2O_2S:Eu^{3+}$	(0.66,0.33)	1.0
$La_2O_2S:Eu^{3+}$	(0.67,0.32)	1.3

respectively. The CIE chromaticity of WL-LED based on $Na_5Eu(WO_4)_2(MoO_4)_2$ and that based on $La_2O_2S:Eu^{3+}$ were found to be (0.29, 0.35) and (0.31, 0.34), respectively. Our results show that both WL-LEDs based on $Na_5Eu(WO_4)_2(MoO_4)_2$ and $La_2O_2S:Eu^{3+}$ show similar luminous efficacy value. Figure 16 shows the color-rendering index variation for WL-LEDs based on n-UV chip, $Na_5Eu(WO_4)_2(MoO_4)_2$, and $La_2O_2S:Eu^{3+}$ operated at a I_f of 20 mA, respectively. The CRI value of the WL-LED of $Na_5Eu(WO_4)_2(MoO_4)_2$ ($Ra \sim 82.3$) was found to be larger than that of the other WL-LED fabricated with commodity of $La_2O_2S:Eu^{3+}$ ($Ra \sim 70.8$) because most of the CRI values for WL-LED based on $Na_5Eu(WO_4)_2(MoO_4)_2$ is larger than those of WL-LED based on $La_2O_2S:Eu^{3+}$, as indicated by Fig. 16. In particular, the CRI no. 9 value of $Na_5Eu(WO_4)_2(MoO_4)_2$ was found to be 82.89, which is apparently much higher and more improved than that using $La_2O_2S:Eu^{3+}$ (−15.20) as a red-emitting phosphor. This CRI no. 9 shows color reproduction quality in the red region. Therefore, $Na_5Eu(WO_4)_2(MoO_4)_2$ was demonstrated to be more suitable for general illumination than $La_2O_2S:Eu^{3+}$. Here, the *R*a value of 82.3 observed for our WL-LED is slightly lower than that of the commodity blue/YAG:Ce^{3+} WL-LED (CRI ~85), presumably because of inherently weak absorption of Eu^{3+} *f-f* transition and the deficient selection of blue or green phosphor. Further improvement is needed to promote the efficiency of our n-UV+blue/green/red WL-LED. In addition, $Na_5Eu(WO_4)_2(MoO_4)_2$ also emit light in the red spectral region under 465 nm blue light excitation (see Fig. 6). For this reason, the red-emitting phosphor can also be combined with the blue chip and YAG phosphor to form one WL-LED with high *R*a value.

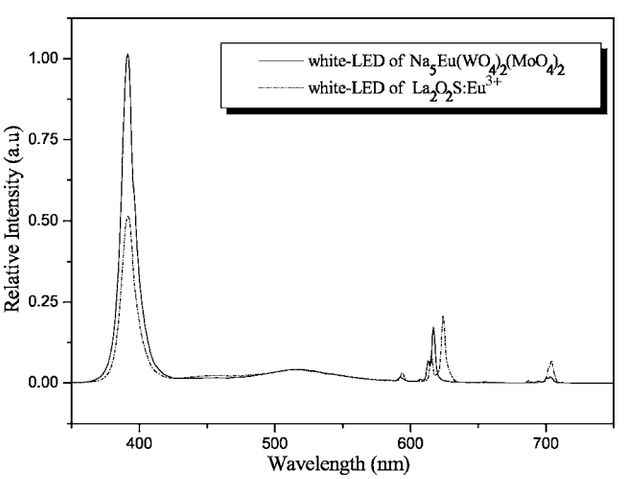

Figure 15. EL spectra of n-UV chip-based WL-LED with $Na_5Eu(WO_4)_2(MoO_4)_2$ and $La_2O_2S:Eu^{3+}$ phosphors and a forward-bias current of 20 mA, respectively.

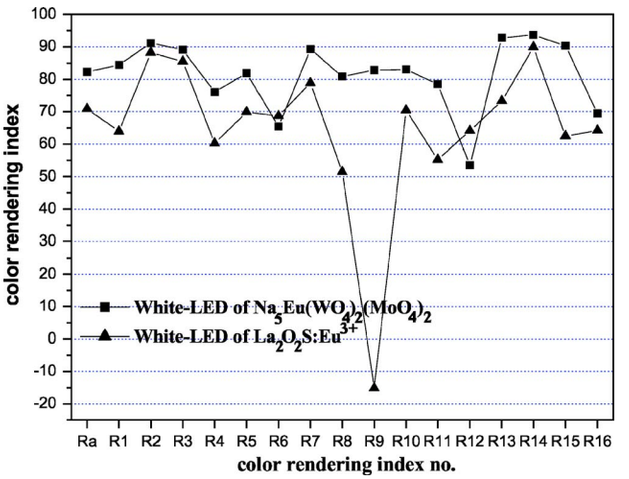

Figure 16. (Color online) CRI variation of WL-LEDs based on n-UV chip, $Na_5Eu(WO_4)_2(MoO_4)_2$ and the commodity of $La_2O_2S:Eu^{3+}$ at a I_f of 20 mA, respectively.

Conclusions

We have prepared a series of red-emitting $M_5Eu(WO_4)_{4-x}(MoO_4)_x$ (M = Li, Na, K) phosphors by high-temperature solid-state reactions. The CIE color coordinates and comparative luminance for the $Na_5Eu(WO_4)_{4-x}(MoO_4)_x$ phosphors have been measured and compared with commodity phosphors of $Y_2O_2S:Eu^{3+}$ and $La_2O_2S:Eu^{3+}$. We have investigated its luminescence properties by integrating an n-UV LED chip, the $Na_5Eu(WO_4)_2(MoO_4)_2$ phosphor and the matching green- and blue-emitting phosphors. The *R*a value of the WL-LED based on $Na_5Eu(WO_4)_2(MoO_4)_2$ was found to be 82.3, higher than that ($Ra \sim 70.8$) of the other WL-LED fabricated using the commodity of $La_2O_2S:Eu^{3+}$. Particularly, the CRI no. 9 value, showing color reproduction in the red region, has been improved from −15.20 to 82.89. In addition, it has also been found that $Na_5Eu(WO_4)_2(MoO_4)_2$ exhibits PL under excitation with a blue-LED chip. Consequently, our research has demonstrated that $Na_5Eu(WO_4)_{4-x}(MoO_4)_x$ exhibits a great potential as a red-emitting phosphor in fabrication of WL-LEDs.

Acknowledgments

This research was supported by funding from National Science Council of Taiwan, under contract no. NSC 95-2113-M-024-MY3.

National Chiao Tung University assisted in meeting the publication costs of this article.

References

1. K. S. Sohn, B. I. Kim, and N. Shin, *J. Electrochem. Soc.*, **151**, H243 (2004).
2. K. Toda, Y. Kawakami, and S. I. Kousaka, *IEICE Trans. Electron.*, **E89–C10**, 1406 (2006).
3. Y. Q. Li, C. A. Delsing, G. de With, and H. T. Hintzen, *Chem. Mater.*, **17**, 3242 (2005).
4. Y. Huh, J. Shim, Y. Kim, and Y. Do, *J. Electrochem. Soc.*, **150**, H57 (2003).
5. Y. Huh, J. Park, S. Kweon, J. Kim, J. Kim, and Y. R. Do, *Bull. Korean Chem. Soc.*, **25**, 1585 (2004).
6. V. Sivakumar and U. V. Varadaraju, *J. Electrochem. Soc.*, **152**, H168 (2005).
7. B. F. Dzhurinskii, L. N. Zorina, G. V. Lysanova, M. G. Komova, N. P. Soshchin, I. V. Tananaev, and E. M. Reznik, *Inorg. Mater.*, **16**, 86 (1980).
8. R. R. Soden, U.S. Pat. 3,183,193 (1965).
9. H. J. Borchardt, U.S. Pat. 32,07,573 (1965).
10. W. H. Dungan, U.S. Pat. 318,095 (1965).
11. H. J. Borchardt, U.S. Pat. 3,328,311(1967).

12. V. K. Trunov, T. A. Berezina, A. A. Evdokimov, V. K. Ishunin, and V. G. Krongauz, *Russ. J. Inorg. Chem.*, **23**, 1465 (1978).
13. J. Huang, J. Loriers, P. Porcher, G. Teste de Sagey, and P. Caro, *J. Chem. Phys.*, **80**, 6204 (1984).
14. N. J. Stedman, A. K. Cheetham, and P. D. Battle, *J. Mater. Chem.*, **4**, 707 (1994).
15. Z. Wang, H. Liang, J. Wang, M. Gong, and Q. Su, *Appl. Phys. Lett.*, **89**, 071921 (2006).
16. S. Neeraj, N. Kijima, and A. K. Cheetham, *Chem. Phys. Lett.*, **387**, 2 (2004).
17. Y. Z. He, X. Y. Huang, and G. F. Wang, *J. Struct. Chem.*, **12**, 346 (1993).
18. V. Sivakumar and U. V. Varadaraju, *J. Electrochem. Soc.*, **153**, H54 (2006).
19. J. A. Blasse and A. Bril, *J. Chem. Phys.*, **45**, 2350 (1966).
20. G. Blasse, *J. Chem. Phys.*, **45**, 2356 (1969).
21. W. Y. Shen, M. L. Pang, J. Lin, and J. Fang, *J. Electrochem. Soc.*, **152**, H25 (2005).
22. J. Pan, L. Yau, L. Chen, G. Zhao, G. Zhou, and C. Guo, *J. Lumin.*, **40-41**, 856 (1988).
23. C. H. Kuo, J. K. Sheu, S. J. Chang, Y. K. Su, L. W. Wu, J. M. Tsai, C. H. Liu, and R. K. Wu, *Jpn. J. Appl. Phys., Part 1*, **42**, 2284 (2003).